ANGLE OF ATTACK OPERATION ZONE ANALYSIS AND DESIGN FOR LIFTING ENTRY

Li Zhaoying, Zhang Rui, Liao Yuxin
School of Astronautics, Beijing University of Aeronautics and Astronautics, Beijing 100191, China
lizhaoying@buaa.edu.cn;zhangrui@buaa.edu.cn;nashlyx2601@yahoo.com.cn

Keywords: *lifting entry vehicle; angle of attack; bank angle; trajectory planning*

Abstract

For lifting entry vehicle, angle of attack is one of the most important trajectory control inputs. This paper aims to develop a practical and effective method for angle of attack design. First, the factors which impact angle of attack are analyzed. The entry flight is discussed as equilibrium glide phase and initial diving phase respectively. And the operation zone of angle of attack is obtained based on constraints of heating rate, aerodynamic load, dynamic pressure and quasi-equilibrium glide condition. An application is given and simulation results show that the proposed angle of attack design method is convenience to obtain angle of attack profile while satisfying all the path constrains.

1 Introduction

Lifting entry is a widely used technique for RLV and CAV. The vehicles are controlled by aerodynamic lift force which enhances the range ability and maneuverability. Angle of attack (AOA for short) and slide angle affect aerodynamic forces mostly. Generally, in entry flight zero slide angle strategy is required for better heating protection. So the design of AOA is one of the most important problems for lifting entry guidance.

For different purposes, a lot of methods have been proposed for AOA optimization and design. For unpowered vehicle, it has been proved that the AOA corresponding to maximum L/D will lead to maximum range without path constraints [1]. The AOA profile is taken as a piecewise function of velocity, the entry range is then optimized by adjusting the velocity at the nodes [2]. Inverse dynamic method is used to solve bank angle and longitudinal trajectory is planned in energy-drag plane. By design different AOA profiles, the guidance commands are obtained for different range [3]. Methods such as pseudospectral and SQP (Sequential Quadratic Programming) can be also used for AOA optimization. However, the convergence and real-time performances of these methods need to be improved. Traditional lifting entry vehicle such like space shuttle uses velocity-AOA profile designed beforehand and the AOA is adjusted slightly during entry flight [4,5].

This paper discusses the factors and constraints which should be considered for AOA design and optimization. Based on QEGC (Quasi-Equilibrium Glide Condition), the lower boundary of AOA is determined. With initial diving strategy AOA profile is designed. This AOA design method is effective in the first stage of vehicle development and production to determine velocity-AOA profile rapidly. The application of footprint problem is given and the simulation results verified the proposed method.

2 Analysis for Angle of Attack

Lifting entry is a multi-constraint task. For entry guidance, heating rate, aerodynamic load and dynamic pressure are three primary hard constraints. Hard constraint means it should not be violated otherwise the vehicle or the crews would be damaged. Besides that, there is equilibrium glide constraint which is soft constraint. It can be violated when necessary

and the vehicle could still be safe. But the trajectory quality might be declined.

The AOA is usually predesigned and adjusted slightly during entry flight. A good nominal AOA profile should consider the factors like thermal protection, aerodynamics, altitude control and navigation while satisfying all the path constraints.

The design of nominal AOA should consider the following factors:

(1) Thermal protection

The heating rate of stagnation point is inversely proportional to the equivalent radius R_s. To reduce heating rate, vehicle always flight with AOA which has maximum R_s. For blunt head entry vehicle, like space shuttle, large R_s comes with big AOA (30deg~50deg).

(2) Height reducing

At the initial part of entry, air density is very thin and provides small aerodynamic forces. If the height of vehicle reduces fast, the heating rate constraint would be violated. To control the height reducing, AOA should be chosen to generate more lift force, and at the same time the drag force also increases to reduce velocity.

(3) Downrange

It has been proved that maximum downrange comes from the AOA which makes lift to drag ratio the maximum value (denoted as $\alpha_{L/D\max}$). So the designed AOA is preferred to be $\alpha_{L/D\max}$ while path constraints are satisfied.

(4) TAEM

When vehicle enters into TAEM (Terminal Area Energy Management) phase, AOA should be less than $\alpha_{L/D\max}$ to keep trajectory stable:

$$\alpha < \alpha_{L/D\max} \qquad (V < V_{\mathrm{TAEM}}) \tag{1}$$

(5) Aerodynamic

Stall AOA is the upper boundary of AOA's operation zone. It is obtained through wind tunnel tests or numerical aerodynamic calculation. AOA should be designed less than stall attack angle with certain margin.

(6) RCS consumption

RCS (Reaction Control System) is used to assist rudder since in high altitude rudder has little efficiency. AOA can be designed to make the distance of mass center and pressure center in an appropriate value and reduces the consumption of RCS. Usually, mass center is closer to pressure center with bigger AOA, and so RCS consumption is smaller.

(7) Short period mode control

Aerodynamic forces are very sensitive to AOA, especially at hypersonic condition. It means slightly adjustment of AOA will bring sufficient control forces. So bank angle is used to control phugoid mode and AOA is to control short period mode. Besides, when bank angle changes the sign, the trajectory will jump instantaneously and AOA is used to compensate. An amended value is added to the nominal attack angle:

$$\alpha = \alpha_{\mathrm{nom}} + \delta\alpha \tag{2}$$

Where α_{nom} is the nominal AOA, $\delta\alpha$ is bounded and typical value for X-33 is $|\delta\alpha| \le 5^\circ$.

(8) Smoothness

For the consideration of control system and aerodynamic stability, AOA profile should be smooth. The first and second order derivatives are bounded:

$$|\dot{\alpha}| \le 2^\circ / s, |\ddot{\alpha}| \le 1^\circ / s^2 \tag{3}$$

3 Angle of Attack Design

3.1 Entry Dynamic

The 3-DOF dimensionless dynamic equations [6] of powerless gliding entry flight are:

$$\begin{cases} \dot{r} = V\sin\gamma \\ \dot{\theta} = V\cos\gamma\sin\psi / r\cos\phi \\ \dot{\phi} = \dfrac{V\cos\gamma\cos\psi}{r} \\ \dot{V} = -D - \dfrac{\sin\gamma}{r^2} + \Omega^2 r\cos\phi(\sin\gamma\cos\phi - \cos\gamma\sin\phi\cos\psi) \\ \dot{\gamma} = \dfrac{1}{V}[L\cos\sigma + \left(V^2 - \dfrac{1}{r}\right)\dfrac{\cos\gamma}{r} + 2\Omega V\sin\psi\cos\phi + \\ \Omega^2 r\cos\phi(\cos\gamma\cos\phi + \sin\gamma\cos\psi\sin\phi)] \\ \dot{\psi} = \dfrac{1}{V}[\dfrac{L\sin\sigma}{\cos\gamma} + \dfrac{V^2\cos\gamma\sin\psi\tan\phi}{r} - \\ 2\Omega V(\tan\gamma\cos\psi\cos\phi - \sin\phi) + \dfrac{\Omega^2 r\sin\psi\sin\phi\cos\phi}{\cos\gamma}] \end{cases} \tag{4}$$

Where r is radial distance from center of the Earth to vehicle and normalized by the radius of the Earth R_0. The longitude and latitude are θ and ϕ. The variable V is the Earth-relative velocity and normalized by $\sqrt{(g_0R_0)}$. g_0 is the gravitational acceleration magnitude on the surface of the Earth. The terms L and D are the aerodynamic lift and drag accelerations in g, which are $L=\rho g_0R_0V^2S_{\text{ref}}C_L/(2mg_0)$ and $D=\rho g_0R_0V^2S_{\text{ref}}C_D/(2mg_0)$. ρ is atmosphere density and S_{ref} is reference area. m is the mass and normalized by initial mass m_0. γ is flight path angle and ψ is velocity azimuth angle. The differentiation is with respect to the dimensionless time $\tau=t/\sqrt{(R_0/g_0)}$. Ω is the Earth self rotation rate normalized by $\sqrt{(R_0/g_0)}$. Bank angle σ and AOA α are usually taken as control inputs.

3.2 Equilibrium Glide Phase

QEGC is a well known flight mechanics for entry guidance. The basis of QEGC is flight path and its rate are small and approximately to zero: $\gamma \approx 0$, $\dot{\gamma} \approx 0$. By ignoring Earth rotation in entry dynamic equations Eq.(4), the QEGC will give following formula:

$$F(\alpha)=(\frac{1}{r}-V^2)\frac{1}{r}-L(\alpha)\cos\sigma=0 \qquad (5)$$

When Eq.(5) is satisfied, the vehicle can equilibrium glide.

The essential principle of lifting entry guidance is: AOA generates lift force and bank angle allocates lift force. From Eq.(5) it can be seen α and σ are compensating each other to keep equilibrium guiding.

With given V, r and σ, the minimum AOA can be find with secant method and noted as α_{EGC}.

$$\alpha_{k+1}=\alpha_k-\frac{F(\alpha_k)(\alpha_k-\alpha_{k-1})}{F(\alpha_k)-F(\alpha_{k-1})} \quad (k=0,1\ldots) \qquad (6)$$

Fig.1 shows the α_{EGC} with different bank angles along the path constraints' lower boundary. It can be explained that the nominal attack angle should be no less than α_{EGC} if bank angle needs 5deg or 40deg control margin. For safety, the AOA also should be bigger than 10deg with high Mach velocity. If necessary, the AOA is allowed to be less than α_{EGC} in a short time.

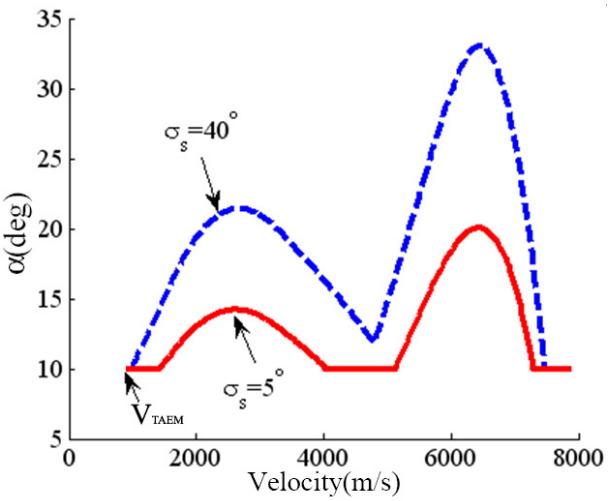

Fig.1. AOA Lower Boundary for Different Bank Angles

3.3 Initial Diving Phase

QEGC holds true while lift force is big enough so aerodynamic forces affect trajectory significantly. For lifting entry, the required lift force to make QEGC available usually happens while the altitude is below 80km. However, there is always a distance from entry interface to the altitude 80km, about 2000km (as shown in Fig.2).

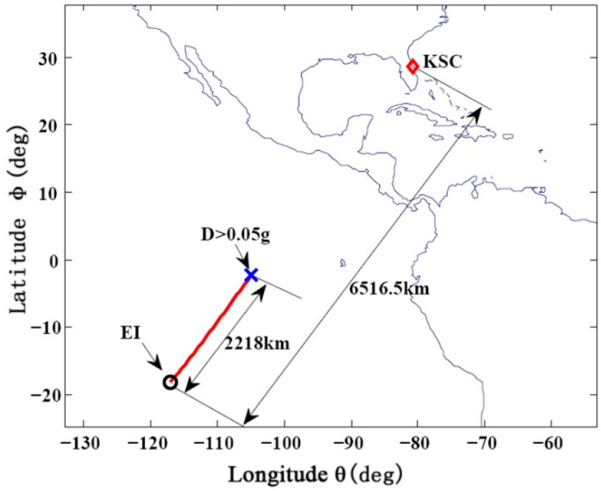

Fig.2. Ground Track from Entry Interface EI to D>0.05g

In the initial diving phase, QEGC doesn't work. To reduce RCS consumption, the vehicle maintains a certain attitude with constant bank angle σ_{InitDsnt} and constant AOA α_{InitDsnt}. Let

$\sigma_{\text{InitDsnt}} = 0$ (that means all the lift force is used to climb), with a initial guess $\alpha^{0}_{\text{InitDsnt}}$, the minimum AOA $\alpha_{\text{InitDsnt\_min}}$ can be obtained through integrating trajectory from entry interface (as shown in Fig.3).

The integration stops while:

$$\frac{\mathrm{d}\dot{Q}(t^*)}{\mathrm{d}t} = 0 \tag{7}$$

A simple way to know whether the Eq.(7) is satisfied is to compare heating rates of time t_n, t_{n-1} and t_{n-2}. If the following conditions are met:

$$\dot{Q}(t_{n-1}) > \dot{Q}(t_n), \dot{Q}(t_{n-1}) > \dot{Q}(t_{n-2}) \tag{8}$$

The integration stops and the search range reduces to $[t_{n-2}, t_n]$. Denote the heating rate at t^* as $\dot{Q}_{\text{trans}}$, and the allowable maximum heating rate as $\dot{Q}_{\max}$. Then the difference between them is:

$$H(\alpha) = \dot{Q}_{\text{trans}} - \dot{Q}_{\max} \tag{9}$$

Using secant method:

$$\alpha_{k+1} = \alpha_k - \frac{H(\alpha_k)(\alpha_k - \alpha_{k-1})}{H(\alpha_k) - H(\alpha_{k-1})} \ (k = 0,1...) \tag{10}$$

The search result is the AOA which makes the trajectory tangent with heating rate boundary (as shown in Fig.3). This AOA is the $\alpha_{\text{InitDsnt\_min}}$, and the velocity at the tangent point is noted as V_{trans}.

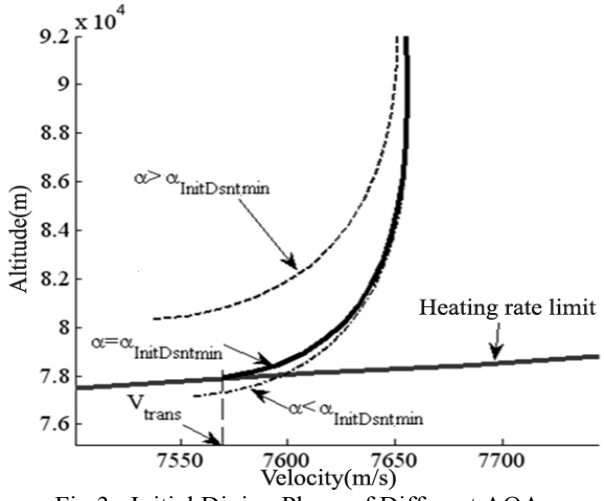

Fig.3. Initial Diving Phase of Different AOAs

3.4 Design Zone

The design zone of AOA is shown as Fig.4.

(1) $\alpha_{\max}$ is the upper boundary of AOA. It is usually obtained by minus safety margin from vehicle's stall AOA.

(2) The lower boundary of AOA is make up of $\alpha_{\text{EGC\_min}}$ and $\alpha_{\text{InitDsnt\_min}}$. $\alpha_{\text{EGC\_min}}$ is found based on path constraints of heating rate, aerodynamic loads and dynamic pressure through Eq.(5). $\alpha_{\text{InitDsnt\_min}}$ is found by integration in section 3.3. For specific velocity the $\tilde{\alpha}_{\min}$ is:

$$\tilde{\alpha}_{\min} = \max(\alpha_{\text{EGC\_min}}, \alpha_{\text{InitDsnt\_min}}) \tag{11}$$

(3) $\alpha_{\text{L/Dmax}}$ is the AOA which makes L/D the maximum value at any given velocity. Theoretically speaking the space between $\alpha_{\max}$ and $\tilde{\alpha}_{\min}$ is the operation zone of AOA. For larger range, the AOA is expected to $\geq \alpha_{\text{L/Dmax}}$. So the is:

$$\alpha_{\min} = \max(\alpha_{L/D\max}, \tilde{\alpha}_{\min}) \tag{12}$$

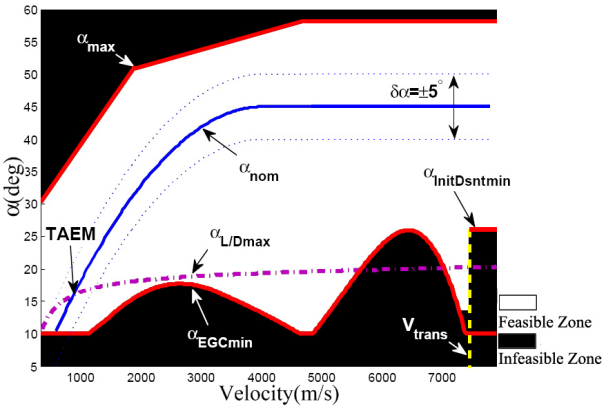

Fig.4. AOA Operation Zone

For practice, the nominal AOA profile can be designed as piecewise quadratic function, which was used in earlier flights of space shuttle:

$$\alpha_{\text{nom}} = \begin{cases} 45 & V > 4000 \\ 45 - 0.262\left(\dfrac{V}{300} - 13\right)^2 & 4000 \geq V \geq V_{\text{TAEM}} \end{cases} \tag{13}$$

Based on Eq.(13), while thermal protection is the primary factor (V>4000m/s), the vehicle flights with large AOA. It helps vehicle reduces velocity and descent slowly. While heating rate is getting better, the vehicle tries to cover larger range and AOA tends to $\alpha_{\text{L/Dmax}}$. The quadratic

function can provide a smooth trajectory (Eq.(3)). While $V=V_{\mathrm{TAEM}}$, α_{nom} and $\alpha_{\mathrm{L/Dmax}}$ intersect. So in TAEM phase the Eq.(1) is satisfied. The $\delta\alpha$ in Eq.(2) is also considered as shown in Fig.4.

If the vehicle has been tested in structure and thermal protection, AOA profile can be designed much closer to $\alpha_{\mathrm{L/Dmax}}$.

For lifting entry trajectory planning, AOA and bank angle are both the control variables. AOA is used to deal with downrange requirement and constraints as described above. Bank angle is used to control the crossrange and final aiming. The operation zones of AOA and bank angle are kind of inverses proportion. When AOA profile is determined, the operation zone of bank angle can also be obtained.

The initial diving bank angle is obtained by the same process as AOA. Like Eq.(9), we can have:

$$H(\sigma)=\dot{Q}_{\mathrm{trans}}-\dot{Q}_{\max} \tag{14}$$

Using secant method to search the constant bank angle:

$$\sigma_{k+1}=\sigma_k-\frac{H(\sigma_k)(\sigma_k-\sigma_{k-1})}{H(\sigma_k)-H(\sigma_{k-1})}\ (k=0,1\ldots) \tag{15}$$

While $|H(\sigma)|$ is less than a certain value, the bank angle is the $\sigma_{\mathrm{InitDsnt\_max}}$.

The upper boundary of bank angle is obtained by:

$$\sigma_{\mathrm{EGC\_max}}=\arccos\left(\frac{(1/r-V^2)/r}{L_{\max}}\right) \tag{16}$$

Here the bank angle operation zone for the AOA profile Eq.(13) is given:

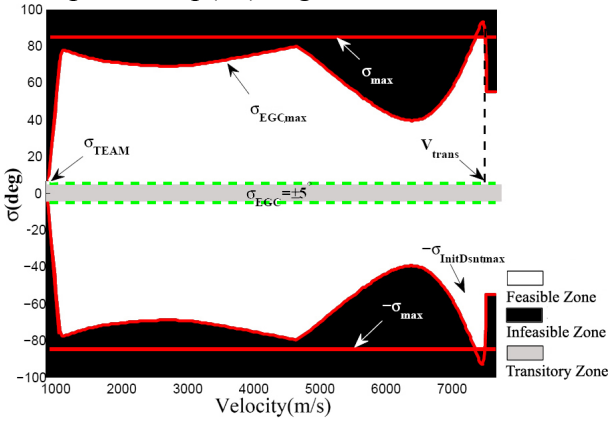

Fig.5. Bank Angle Operation Zone

The subscripts in Fig.5 have the same meaning of Fig.4. The transitory zone is control margin for online guidance system. In trajectory planning, the bank angle should not be stay in this zone for a long time.

4 Simulation and Verification

To verify the proposed AOA profile design method, simulations of X-33 entry flight is given.

The nominal AOA profile of X-33 is:

$$\alpha_{\mathrm{nom}}=\begin{cases}45 & 10\le Ma\le 26\\ 45-0.612(Ma-10)^2 & 3.5\le Ma\le 10\end{cases} \tag{17}$$

The test parameters are shown in Table 1.

Table 1 Simulation Parameters

	Meaning	Value
Position	Longitude(deg)	242.993
	Latitude(deg)	-18.355
	Altitude(km)	121.518
Velocity	Velocity(m/s)	7622
	Flight path angle(deg)	-1.438
	Heading angle(deg)	38.329
Path constraints	Heating rate(W/m^2)	680935
	Load(g)	2.5
	Dynamic pressure(N/m^2)	14364

First, the AOA operation zone is obtained and then different AOA profiles are calculated through linear interpretation from α_{nom} to $\alpha_{\min}$ (as shown in Fig.6).

$$\alpha=k\alpha_{\mathrm{nom}}+(1-k)\alpha_{\min}\quad k\in[0,1] \tag{18}$$

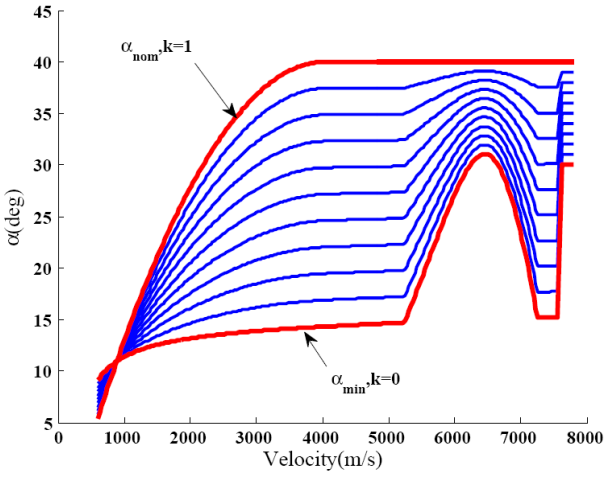

Fig.6. AOA Profiles

For each AOA profile, bank angle control law in Ref.[7] is applied. The corresponding bank angle commands are obtained (Fig.7). It can be found that the smaller AOA profile is, the smaller upper boundary of bank angle is. Because small AOA will result in small lift force in longitudinal plane, in order to maintain equilibrium gliding the bank angle should be small.

Fig.8 shows that all the entry trajectories satisfy path constraints and reach intersection point of TAEM.

Fig.9 is the heating rate for different AOA profiles. Dashed line is heating rate constraint. The smaller AOA is, the longer time vehicle flies. When AOA getting small the peak value of heating rate doesn't reduce, it means that smaller AOA results to greater total heat.

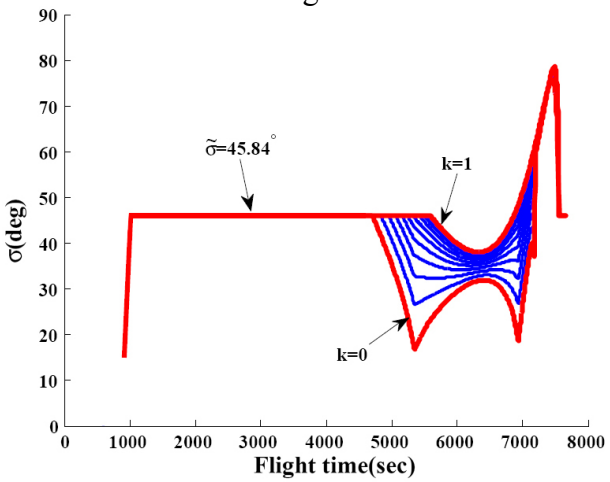

Fig.7. Bank Angle Profiles

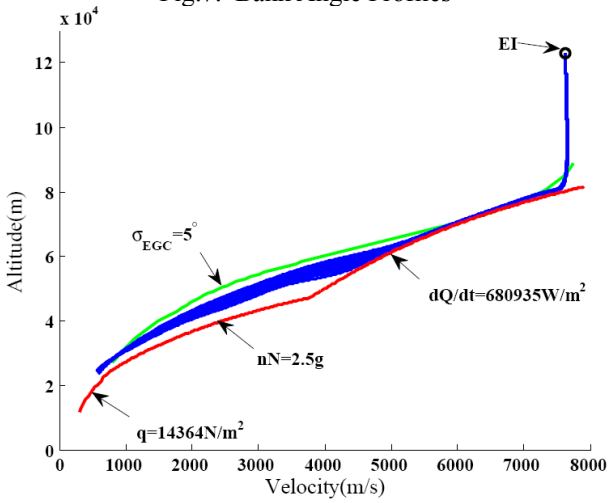

Fig.8. Trajectories of Different AOA Profiles

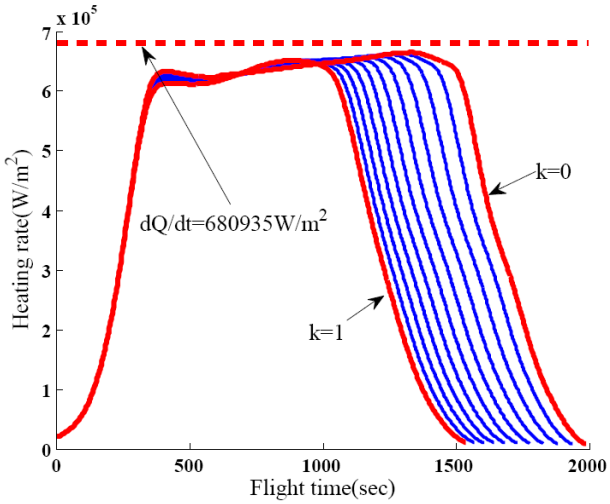

Fig.9. Heating Rate of Different AOA Profiles

Fig.10 shows the application of footprint problem. The footprints of different AOA profiles are obtained with the same constraints and conditions. The k is the design parameter in Eq.(18). The value of k is related to the area of footprint. It can be seem from Fig.10, the AOA profile affects range capability of vehicle significantly.

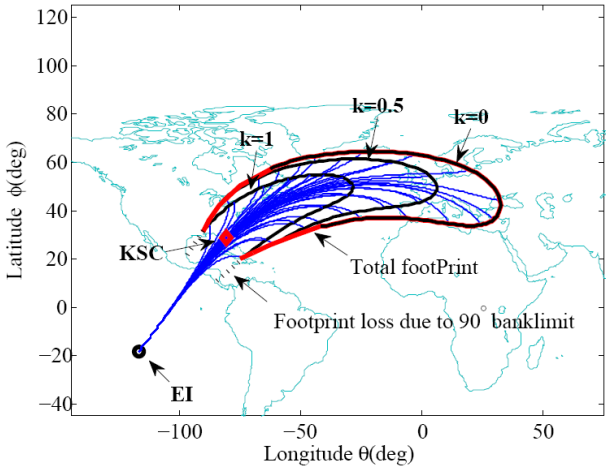

Fig.10. Footprint with Different AOA Profiles

5 Conclusion

A method for AOA profile design is proposed for lifting entry. The method considers many engineering factors and path constraints. QEGC is used to obtain the operation zone of AOA. The AOA profile design is simplified to a parameter search problem in a given space. The simulation shows that this method can be used to quickly determine V-α profile which satisfies all the path constraints. The application of

footprint problem also demonstrates the feasibility of this method.

References

[1] Vinh N X. *Optimal trajectories in atmospheric flight*. Elsevier Scientific Publishing Company, NewYork, 1981.

[2] Yong E M, Tang G J, Chen L. Rapid trajectory planning for hypersonic unpowered long-range reentry vehicles with multi-constraints. *Journal of Astronautics*, Vol. 29, No. 1, pp 46-52, 2008.

[3] Amitabh S, James A, Leavitt and Kenneth D. Landing footprint computation for entry vehicles. *AIAA Guidance, Navigation, and Control Conference and Exhibit*, Providence, Rhode Island, 2004.

[4] Harpold J C, Graves C A. Shuttle entry guidance. *The Journal of the Astronautical Sciences*, Vol. 37, No. 3, pp 239-268, 1979.

[5] Wayne H J, Nicole O L and Timothy W G. Operational experience with hypersonic flight of the space shuttle. *NASA Report*, 17-5259.

[6] Shen Z, Lu P. On-board generation of three-dimensional constrained entry trajectories. *Journal of Guidance Control and Dynamics*, Vol. 26, No. 1, pp 111-121, 2003.

[7] Xue S B, Lu P. Constrained predictor–corrector entry guidance. *Journal of Guidance, Control, and Dynamics*, Vol. 33, No. 4, pp 1273-1281, 2010.

Copyright Statement